Dual-Polarization Beamforming Techniques for Multipath Mitigation in GNSS Handheld Receivers

Lucía Pallarés-Rodríguez, Gonzalo Seco-Granados, José A. López-Salcedo

Signal Processing for Communications and Navigation (SPCOMNAV)
Department of Telecommunication and Systems Engineering
Universitat Autònoma de Barcelona (UAB), IEEC-CERES, Barcelona, Spain

Abstract—This paper analyses the impact of exploiting polarization diversity for multipath mitigation in GNSS handheld receivers. While the use of array processing techniques has been widely studied in the field of multipath mitigation, few studies consider receivers equipped with very small antenna arrays, which is the case of handheld devices. When working with few antennas some performance limitations appear due to the small size of the array, so these must be counteracted by exploiting additional information available at the receiver. One possible solution is to make use of polarization diversity, taking advantage of the fact that in most multipath scenarios, reflected replicas tend to have a different polarization from that of the desired signal. Therefore, this paper evaluates the performance of some array processing techniques when combined with dual-polarized antennas, showing that the small size of the array can be effectively counteracted by exploiting polarization diversity when combating multipath.

Index Terms—GNSS, Array processing, Beamforming, Multipath mitigation, Dual-polarization.

I. INTRODUCTION

Global Navigation Satellite Systems (GNSS) have become a key element in many applications, both in the civilian and industrial scope. The scenarios in which these systems operate are typically hostile, and the propagation impairments that appear tend to degrade the quality of the signal, ultimately leading to inaccuracies in the positioning solution. In this field, multipath is usually identified as one of the major threats in these applications, as the intrinsic characteristics of GNSS signals makes them vulnerable to the presence of highly correlated replicas. The presence of multipath distorts the code correlation computed at the receiver, hindering the correct computation of the code delay and carrier phase. Numerous approaches have been proposed in order to mitigate the undesired effects these reflections cause. Some of them operate at a receiver level, modifying the conventional scheme of GNSS receivers, for instance, through the use of narrow correlators that provides robustness in the correlation operation [1], or taking advantage of additional parameters that may contain multipath information, such as the C/N_0 [2]. Moreover, the miniaturization tendency of components experienced during the last decades has opened the door to the employment of novel techniques that entail the deployment of

additional hardware components in the receiver, as it is the case of antenna arrays [3].

The use of multiple antennas, also known as beamforming, has been present in the wireless communications area for some time, being nowadays a standardized characteristic in many communication schemes through the use of multiple-input, multiple output (MIMO) systems [4]–[6]. The promising results observed in this field has motivated the adoption of similar techniques in different fields where exploiting the spatial domain could acutely improve the receiver performance, as it is the case of GNSS receiver. Acquiring spatial information about the impinging signals allows the implementation of advanced techniques that intend to maintain the desired contribution coming directly from the satellites, i.e. line-of-sight signal (LOSS), and try to mitigate additional components that may degrade the performance. However, contrary to the wireless communication scenario, where the deployment of several antennas is feasible due to the high operating frequencies of such technologies that results in millimeter-wave signals, the frequency range in GNSS highly restricts the number of usable antennas. As the inter-element separation for the correct functioning of the array is driven by half the signal wavelength, the space needed to deploy multiple antennas in GNSS devices, where the signal carrier wavelength is on the order of a few decimeters, is enlarged with respect to other technologies. One may think that reducing the elements separation could solve the space constraint, but this will lead to ambiguities in the array response (similar to the aliasing effect in the frequency domain), limiting the performance of the array.

This problem is accentuated when discussing handheld devices, such as smartphones and tablets, a group that constitutes great part of the available GNSS receivers [7]. In this arena the space restrictions are emphasized due to the trend towards smaller devices, where locating several antennas while respecting the required inter-element separation entails a challenge. These constraints leave the only possibility of placing very few antennas in order to exploit spatial diversity, two in the case of smaller receivers and up to four in the best cases, which inevitably affects the performance of the implemented techniques and their mitigation capacity. At this point, the need arises to provide additional information as a means to fight the inherent limitations of small antenna arrays

and improve the performance of the receiver in the presence of correlated sources. Innovative beamforming techniques, combine the use of both spatial and temporal references available at the receiver, contrary to more traditional approaches where just one of these is exploited. The combination of the direction of arrival (DoA) of the LOSS along with the reference signal available at the receiver, i.e., PRN code, leads to more robust techniques that improve the performance of the receiver, especially in challenging circumstances.

Nevertheless, in the context of multipath mitigation, further information can be used to equip the techniques with higher capacities. GNSS signals are right hand circularly polarized (RHCP), but when it is reflected from a surface, the polarization of the resulting ray will be modified if the incident angle exceeds the Brewster angle [8], [9]. Several studies have been conducted in order to model multipath in GNSS applications, showing that multipath signals do have significant incident angles and therefore supporting the previous statement [10]–[12]. Considering this, some multipath mitigation approaches exploiting array antennas consider the use of dual-polarized antennas to extract this valuable information from the impinging replica. Some examples can be found in [13]–[15]. The purpose of this paper is therefore to analyse the introduction of polarization diversity in some existing beamforming techniques in order to provide the receiver with reinforced mitigation capabilities against multipath without having to modify the receiver architecture.

The remaining paper is organized as follows. Section II presents the signal model that will be employed thorough the paper, taking into account the case of dual-polarized sensors, as well as the basic concepts on array processing. Section III offers a brief description of the beamforming techniques under study, and Section IV shows the simulations results obtained. Lastly, the conclusions of this work are reported in Section V.

II. SIGNAL MODEL AND PROBLEM STATEMENT

A. Signal Model

Let us consider an array with L elements receiving a LOSS coming directly from the satellite along with M multipath replicas consequence of the reflection of the LOSS in nearby objects. The resulting combination of signals perceived by the L antennas can be therefore expressed through a $L \times 1$ vector, $\mathbf{x}(n)$, with the following complex baseband signal representation,

$$\mathbf{x}(n) = \alpha_0 \mathbf{a}(\theta_0)s(n; \tau_0, \varphi_0) + \sum_{m=1}^{M} \alpha_m \mathbf{a}(\theta_m)s(n; \tau_m, \varphi_m) + \mathbf{n}(n) \tag{1}$$

with $s(n; \tau, \varphi)$ the samples at the output of the GNSS code correlator, containing the correlation peak affected by some time delay τ and carrier phase φ. The amplitude of the received signal, including the attenuation encompassing the propagation losses, is represented by α. The spatial signature is denoted by $\mathbf{a}(\theta) \in \mathbb{C}^{L \times 1}$ and it is introduced by the array for a signal coming from direction θ. Note that the subscript $_0$ in (1) is used to refer to the LOSS, whereas $_m$ denotes the parameters

corresponding to the different multipath reflections. Lastly, the term $\mathbf{n}(n) \in \mathbb{C}^{L \times 1}$ models the noise at each antenna channel.

The signal model in (1) represents the samples received at each antenna of the array after correlation with the local replica of the GNSS signal. This approach is consistent with the fact that GNSS signals are buried below the noise floor when they arrive at the antenna array, but they emerge and become clearly visible once the despreading takes place. Working at post-correlation is therefore convenient when GNSS multipath mitigation is being targeted. In this work we will assume that such post-correlation samples are obtained by correlating the received signal with a local replica driven by a delay-locked loop (DLL) and whose carrier is being wiped off by a phase-locked loop (PLL). This means to work at the tracking stage of the GNSS receiver by having both the DLL and PLL running while the post-correlation samples are obtained and thus, while beamforming is being applied. This is an important consideration because it implies that beamforming will have an impact on the GNSS signal tracking, and therefore the performance analysis to be conducted will need to account for this as well.

In the case that the array antennas are linearly polarized, the spatial signature, i.e, the steering vector of the array, takes the form shown in (1). However, when using dual polarized antennas the existing polarization diversity is contemplated in the steering vector, in such a way that we can differentiate the output of the RHCP channel from that of the LHCP channel. The signal model will thus take the form shown in (2), where only one multipath replica is considered.

$$\mathbf{x}_R(n) = \alpha_0 \mathbf{a}_R(\theta_0)s(\tau_0, \varphi_0) + \alpha_m \mathbf{a}_R(\theta_m)s(\tau_m, \varphi_m) + \mathbf{n}_R(n)$$
$$\mathbf{x}_L(n) = \alpha_0 \mathbf{a}_L(\theta_0)s(\tau_0, \varphi_0) + \alpha_m \mathbf{a}_L(\theta_m)s(\tau_m, \varphi_m) + \mathbf{n}_L(n) \tag{2}$$

With the purpose of generality, the steering vectors in (2) are defined assuming that the multipath reflection may arrive with elliptical polarization, a combination of both RHCP and LHCP, and hence it will be present in both channels. The steering vectors will then become,

$$\mathbf{a}_R(\theta_i) = \begin{bmatrix} a_R^1 \gamma_R^i \rho \\ a_R^2 \gamma_R^i \rho \\ \vdots \\ a_R^M \gamma_R^i \rho \end{bmatrix} \quad \mathbf{a}_L(\theta_i) = \begin{bmatrix} a_L^1 \gamma_L^i \rho \\ a_L^2 \gamma_L^i \rho \\ \vdots \\ a_L^M \gamma_L^i \rho \end{bmatrix} \tag{3}$$

parameter $\gamma_{R,L}^i$ in (3) models the portion of the i-th signal that arrives with each polarization. Additionally, the cross-talk between both channels is also reflected in the steering vectors depicted in (3) through ρ. With the previous description, and taking into account the following definitions,

$$\mathbf{x}(n) = \begin{bmatrix} \mathbf{x}_R(n) \\ \mathbf{x}_L(n) \end{bmatrix} \quad \mathbf{a}(\theta_i) = \begin{bmatrix} \mathbf{a}_R(\theta_i) \\ \mathbf{a}_L(\theta_i) \end{bmatrix} \tag{4}$$

equation (2) can be rewritten as,

$$\mathbf{x}(n) = \alpha_0 \mathbf{a}(\theta_0)s(\tau_0, \varphi_0) + \alpha_m \mathbf{a}(\theta_m)s(\tau_m, \varphi_m) + \mathbf{n}(n) \tag{5}$$

where it can be seen that the size of the received signal $\mathbf{x}(n)$ when dual polarized antennas are used is dictated not by the number of antennas in the array but by the total number of channels. This results in, considering a RHCP and LHCP channel per antenna, a signal at the input of the beamformer of size $2L \times 1$.

B. The Beamforming Principle

Beamforming is the result of linearly combining the signal samples received at each of the antennas in the array in such a way that it satisfies a predefined criteria established by the technique employed. Most beamforming techniques aim to concentrate the array beam towards the DoA of the LOSS while minimizing the contributions arriving from other directions. This is done by applying a set of coefficients or *weights* previously computed to fulfill the design criteria, to the incoming signal in (5). The result is,

$$y(n) = \mathbf{w}^H \mathbf{x}(n) \tag{6}$$

where $\mathbf{w}$ is the weight vector and $y(n)$ is the signal at the beamformer output. As can be seen, the coefficients in the weight vector are applied to the outputs of each antenna, meaning that the dimensions of $\mathbf{w}$ will be given by those of the input signal. In particular, for the case of dual-polarized antennas, the weight vector will take the form,

$$\mathbf{w} = \begin{bmatrix} \mathbf{w}_R \\ \mathbf{w}_L \end{bmatrix} \tag{7}$$

where $\mathbf{w}_R$ contains the weights applied to the RHCP channels and $\mathbf{w}_L$ contains those for the LHCP outputs.

III. BEAMFORMING TECHNIQUES

The power of beamforming resides in how the weights are computed, which is the essence of any given technique. The most common approaches rely on having prior knowledge about the DoA of the LOSS, which can be obtained through spectral estimation methods [16], [17], maximum likelihood estimation [18] or, in the case of GNSS, through the satellite's ephemeris and the orientation of the receiver. For the remaining of this paper, the DoA of the LOSS will be assumed to be known for those techniques that require its use.

A. Capon Beamformer

The *Capon* beamformer (CAP), also known as *minimum variance distortionless response* (MVDR), is the most general beamforming approach. The technique is formulated by minimizing the power of the signal at the output of the beamformer while keeping a unitary gain at the desired DoA. This constraint introduced at the DoA of the LOSS is the so-called distortionless constraint, as it avoids the mitigation of the desired source, and leads to the following minimisation problem,

$$\min_{\mathbf{w}} P_y = \min_{\mathbf{w}} \mathbf{w}^H \mathbf{R_x} \mathbf{w} \text{ subject to } \mathbf{w}^H \mathbf{a}(\theta_0) = 1 \tag{8}$$

where $\mathbf{R_x} \doteq \mathrm{E}\left[\mathbf{x}(n)\mathbf{x}(n)^H\right] \in \mathbb{C}^{L \times L}$ is the auto-correlation matrix of the data in $\mathbf{x}(n)$, and the term $\mathbf{w}^H \mathbf{a}(\theta_0) = 1$ is the distortionless response constraint. Through the use of Lagrange multipliers, the weights $\mathbf{w}_{CAP}$ become [16],

$$\mathbf{w}_{\mathrm{CAP}} = \frac{\mathbf{R_x}^{-1} \mathbf{a}(\theta_0)}{\mathbf{a}(\theta_0)^H \mathbf{R_x}^{-1} \mathbf{a}(\theta_0)}. \tag{9}$$

B. Eigen-Beamformer

The term *Eigen-beamformer* is used to group an extended family of techniques that solve the proposed optimization problem through the eigenvalues corresponding to the signal space. In this paper, the Eigen-beamformer presented in [19] is evaluated. Here the power of the undesired contributions at the output of the beamformer is minimised, while maintaining the power corresponding to the LOSS through a constraint. This leads to the following formulation,

$$\min_{\mathbf{w}} \mathbf{w}^H \left(\mathbf{R_m} + \mathbf{R_n}\right) \mathbf{w} \text{ subject to } \mathbf{w}^H \left(\mathbf{R_s} + \mathbf{R_n}\right) \mathbf{w} = \Phi \tag{10}$$

where $\mathbf{R_m}$ is the auto-correlation matrix corresponding to the multipath contributions, $\mathbf{R_n}$ is the noise covariance matrix, $\mathbf{R_s}$ is the auto-correlation matrix of the desired signal, and Φ is the value of the power constraint. Estimating $\mathbf{R_m} + \mathbf{R_n} \approx \mathbf{R_x} - \mathbf{R_s}$, the optimum solution to the previous optimization problem is given by,

$$\mathbf{w}_{\mathrm{EIG}} = \mathcal{P}\left\{\left(\mathbf{R_x} - \mathbf{R_s}\right)^{-1}\left(\mathbf{R_s} + \mathbf{R_n}\right)\right\} \tag{11}$$

where operator $\mathcal{P}\{\cdot\}$ retrieves the principal eigenvector of the matrix.

C. Linear Minimum Mean Square Error Beamformer

The *linear minimum mean square error* (LMMSE) beamformer exploits the temporal reference of the desired signal available at the receiver, in the particular case of GNSS, the PRN code used for despreading. Therefore, the LMMSE is formulated through the minimisation of the mean square error (MSE) between the received signal and the locally generated replica, $s(\tau, \varphi)$. The solution to this problem is given by [20],

$$\mathbf{w}_{\mathrm{LMMSE}}(\tau_0, \varphi_0) = \mathbf{R_x}^{-1} \mathbf{r_{xs}}(\tau_0, \varphi_0) \tag{12}$$

with $\mathbf{r_{xs}}(\tau, \varphi) \doteq \mathrm{E}\left[\mathbf{x}(n)s^*(\tau, \varphi)\right] \in \mathbb{C}^{L \times 1}$ the cross-correlation between the array output and reference signals.

D. LMMSE-Capon Hybrid Beamformer

As briefly introduced in section I, some beamforming techniques combine the use of a spatial and temporal reference, leading to more refined techniques that improve the performance of the receiver at the expense of a slightly higher complexity. This is the case of the LMMSE-Capon Hybrid beamformer, a linear combination of the Capon and LMMSE beamformers [21]. Incorporating both spatial and temporal references translates into higher multipath mitigation capacities, compensating the deficiencies that each techniques

presents individually. The solution for the optimum weights is then given by,

$$\mathbf{w}_{\text{HYB}}(\tau_0, \varphi_0) = \alpha_0^* \mathbf{w}_{\text{LMMSE}}(\tau_0, \varphi_0) + \beta(\tau_0, \varphi_0)\, \mathbf{w}_{\text{CAP}} \quad (13)$$

where $\beta(\tau_0, \varphi_0) \doteq 1 - \alpha_0^* \mathbf{a}^H(\theta_0)\mathbf{w}_{\text{LMMSE}}(\tau_0, \varphi_0)$

E. Power-based Capon Beamformer

In the presence of multipath reflections, the traditional Capon beamformer presents an undesired behaviour due to the high correlation between the LOSS and the impinging replicas. In this case, matrix $\mathbf{R_x}$ is composed by the auto-correlation matrix of each of the individual signals as well as additional cross-correlation terms resulting from the correlation between the multipath contribution and the LOSS. The presence of these terms in the auto-correlation matrix $\mathbf{R_x}$ causes the Capon beamformer to mix these contributions when minimising the power at the output, thus leading to an undesired cancellation of the LOSS. In that sense, the *Power-Based Capon Beamformer* (PBC) overcomes this limitation by estimating the value of the cross-correlation terms and subsequently removing them from the auto-correlation matrix. This results in a modified version of the Capon beamformer, where the matrix $\mathbf{R_x}$ indicated in (9) is replaced by an altered version, $\tilde{\mathbf{R}}_\mathbf{x}(\tau_0, \varphi_0)$, obtained as follows [22],

$$\boldsymbol{\Gamma}_\mathbf{x}(\tau_0, \varphi_0) = \mathbf{a}(\theta_0)\boldsymbol{\kappa}(\tau_0, \varphi_0)^H + \boldsymbol{\kappa}(\tau_0, \varphi_0)\mathbf{a}^H(\theta_0) \quad (14)$$

where $\boldsymbol{\kappa}(\tau_0, \varphi_0) \doteq \alpha_0 \mathbf{r_{xs}}(\tau_0, \varphi_0) - \alpha_0^2 \mathbf{a}(\theta_0)$. Then, defining the new auto-correlation matrix $\tilde{\mathbf{R}}_\mathbf{x}(\tau_0, \varphi_0) \doteq \mathbf{R_x} - \boldsymbol{\Gamma}_\mathbf{x}(\tau_0, \varphi_0)$, the PBC is given by,

$$\mathbf{w}_{\text{PBC}} = \frac{\tilde{\mathbf{R}}_\mathbf{x}^{-1}(\tau_0, \varphi_0)\mathbf{a}(\theta_0)}{\mathbf{a}(\theta_0)^H \tilde{\mathbf{R}}_\mathbf{x}^{-1}(\tau_0, \varphi_0)\mathbf{a}(\theta_0)} \quad (15)$$

IV. PERFORMANCE EVALUATION

This section is aimed at shedding light onto the performance of the aforementioned beamforming techniques when deployed into a small-size antenna array. This would actually be the case of a smartphone- or a table-like device. The emphasis is then placed on the availability of an additional degree of freedom, which is given by the use of dual-polarized antennas. The overall goal is to analyze up to which extent the use of such additional degree of freedom can compensate the reduced dimensionality in the spatial domain. As a baseline, results for the case of linearly polarized antennas are offered, in order to provide a reference of the expected capabilities in the case no polarization diversity is exploited.

A. Simulation set-up and performance metrics

For the comparison of the different configurations and techniques, the performance is evaluated through three main metrics that allow to characterize the robustness provided by the beamformers in each case. The first metric is the *array response* (AR), defined in (16) as the ratio between the array factor at the DoA of the multipath and at the DoA of the LOSS.

This parameter allows to evaluate the signal-to-multipath ratio (SMR) at the output of the beamformer, as the AR establishes the relationship between the power received from the DoA of the multipath replica and from the DoA of the signal of interest, thus offering an insight of the amount of power from the reflection that is still present after applying the weights.

$$\text{AR}(\theta_m) = 10 \log_{10}\left(\frac{|\mathbf{w}^H \mathbf{a}(\theta_m)|^2}{|\mathbf{w}^H \mathbf{a}(\theta_0)|^2}\right) \quad [\text{dB}] \quad (16)$$

However, for a correct characterization of the performance, additional metrics that better reflect the overall performance of the receiver must be defined. In this sense, valuable information can be extracted from the output of the DLL and PLL, as they reflect the impact that the remainder multipath contribution has on the positioning solution, as well as on the tracking of the LOSS. For the simulation results presented a normalized dot product DLL discriminator with an early-late spacing of 1 chip was used, along with a four-quadrant arctangent discriminator in the case of the PLL. With the previous configuration, the root-mean-square error (RMSE) of the output of these loops constitute the two remaining metrics exploited in this analysis.

The scenario to be considered herein comprises a LOSS affected by a single multipath ray, which is a simple enough while often effective model to analyze the receiver tracking performance [23]. It will be assumed that the LOSS is received at 45 dB-Hz C/N_0, whereas the replica arrives with half the power of the LOSS, $C/N_0 = 42$ dB-Hz. Considering the elliptical nature of multipath reflections, a ρ factor of $\sqrt{1/2}$ has been assumed for the simulations, considering that the total power of the ray is equally divided between both polarizations. Additionally, a cross-talk factor between channels (γ) of 10 dB has been fixed for the characterization. The LOSS and the replica are considered to impinge the array from $10°$ and $30°$ elevation respectively, keeping an azimuth in both cases of $30°$.

B. Antenna Array Configuration

As the purpose of this paper is to evaluate the use of dual polarized arrays in handheld receivers, the space limitations imposed by these devices need to be taken into consideration. Following this, a two-element uniform linear array (ULA2) and a four-element uniform rectangular array (URA4) have been considered for the simulations, analysing in each case three different antenna array polarizations: linearly polarized antennas, RHCP antennas and dual-polarized antennas.

In the case of dual-polarized antennas, the maximum number of output channels has been set to four, following a design criteria feasible for handheld devices. In this sense, the ULA2 array provides, for each antenna element, both RHCP and LHCP outputs, resulting into four channels to be processed. However, for the URA4 configuration, the same approach would lead to a total of eight channels to be simultaneously processed, thus requiring an excessive complexity that is out of reach of most COTS devices. It is for this reason
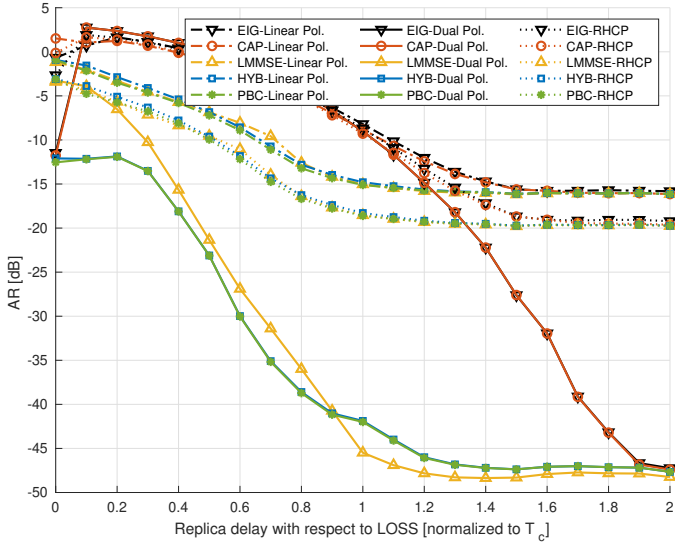
Fig. 1: AR for the different array polarizations in the ULA2 configuration.

Fig. 2: RMSE for the different polarizations in the ULA2 configuration for the DLL (top) and for the PLL (bottom).

that for the URA4 configuration, whose antennas are placed forming a square, only one output port is considered from each antenna. In particular, only the RHCP output is processed for antennas placed along one diagonal while only the output from the LHCP channel is considered for the antennas along the opposite diagonal.

C. Simulation Results

The results presented in this paper have been obtained with the configurations previously described, while sweeping over different values for the replica delay. The closer in time the multipath reflection arrives at the receiver with respect to the LOSS, the harder it will be for the receiver to distinguish both, and it will therefore lead to larger undesired effects. These small values for the time delay of the multipath are those that hinder the accuracy of the positioning solution the most, hence it is in these near replicas where the attention must be focused. For this reason, with the aim of evaluating the impact that the time delay has on the different array configurations, values for the replica delay from 0 to 2 chips with respect to the LOSS and normalized to the chip period (T_C) have been considered, studying the evolution of the three proposed metrics.

Fig. 1 shows the AR of the techniques described in Section III when implemented in the ULA2 array, while Fig. 2 presents the RMSE for both DLL and PLL with the same configuration. The performance exhibited by the HYB, PBC and LMMSE beamformers in terms of cancellation of the replica is considerably better than that of the EIG and CAP beamformers. This is due to the similar nature that the last two techniques present, they both minimize the power at the output of the array disregarding the cross-correlations terms. These terms are those that most degrade the performance of the receiver in the presence of multipath, and thus neglecting them causes the malfunction observed with these two approaches. In this line, the techniques that make use of the local replica of
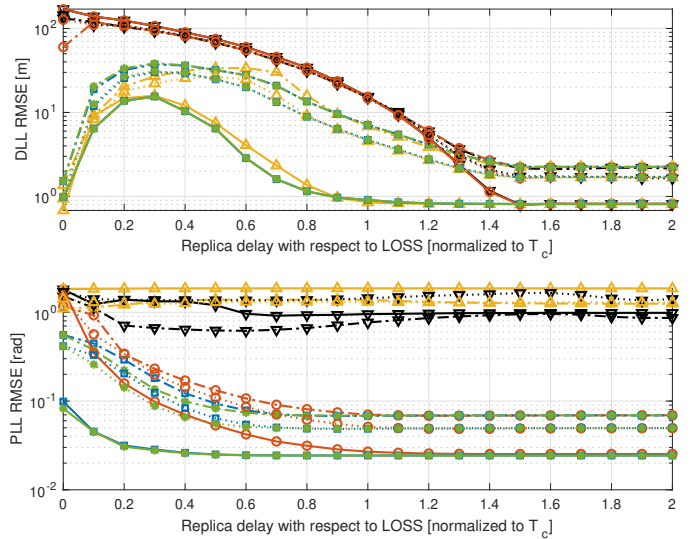
the PRN code, as it is the case of the HYB, PBC and LMMSE present superior mitigation capacity.

The cancellation effect perceived in the EIG and CAP for small replica delays, where the AR ratio is positive, does not apply for the algorithms exploiting temporal references, as they are all unaffected by the cross-correlation contributions. The minimization of the MSE formulated for the LMMSE beamformer guarantees an optimum solution for the weights whenever the local replica is accurate, and hence it shows promising results in terms of mitigation capacity even with highly correlated replicas. However, in Fig. 2 it can be seen that this approach presents poor performance in terms of PLL. Here, the RMSE is higher than for those techniques that are derived imposing a distortionless constraint in the array response. This restriction enables a good tracking performance, as it guarantees that no phase jumps are introduced in the application of the weights, and therefore allowing the correct functioning of the PLL. With this information, it can be seen that the most effective approaches are the techniques that combine both temporal and spatial references, the HYB and PBC, which obtain very high cancellation of the reflection while keeping both the DLL and PLL RMSE very low.

When comparing the results obtained with the different polarization schemes under analysis it can be seen that those algorithms that exhibit a favorable performance, the HYB and PBC, significantly increase their performance when dual-polarized antennas are employed. For instance, when using the HYB or the PBC along with polarization diversity the mitigation capacity is improved in approximately 10 dB for very small replica delays with respect to the case of linearly polarized antennas, and around 7 dB with respect to the circularly polarized array. This difference in the cancellation of the replica is accentuated as the delay of the replica takes larger values, since the correlation between multipath and
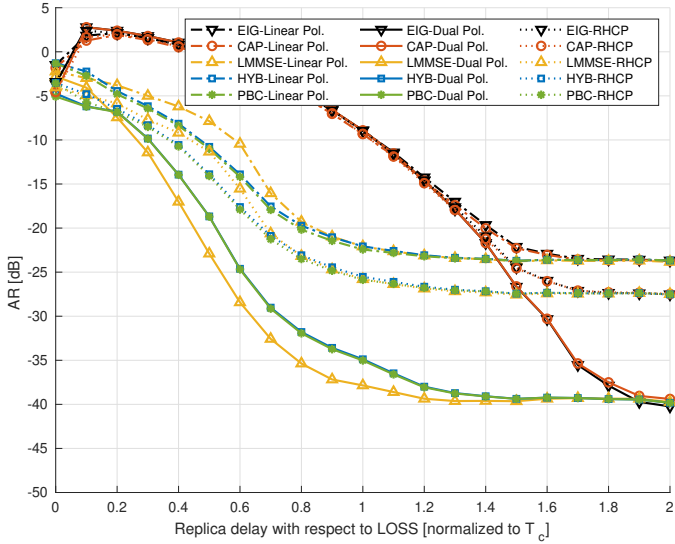
Fig. 3: AR for the different array polarizations in the URA4 configuration.

Fig. 4: RMSE for the different polarizations in the URA4 configuration for the DLL (top) and for the PLL (bottom).

LOSS decreases with this increment, but the most interesting result is observed for very small delays, less than $0.5T_c$, which are the most difficult to counteract.

The positive impact that dual-polarized antennas have on the receiver performance is also supported by the results obtained for the PLL and DLL errors, depicted in Fig. 2. An accurate positioning solution is strongly dependent on a correct time-delay estimation from the DLL. In this sense, exploiting polarization diversity in the array improves the LOSS time delay estimation in around 15 meters with respect to the linearly polarized array and around 10 meters when comparing the results with those of the circularly polarized antennas. Note that these values are achieved for highly correlated replicas, spaced from the LOSS by less than half a chip, and thus showing great improvement in those scenarios where the impact of multipath is critical.

The results presented in Fig. 3 and Fig. 4 show the performance obtained for the URA4 array. Overall, the results do not differ as much as they do in the ULA2 case when comparing the different antenna polarization schemes, although it is still noticeable that the use of dual-polarized antennas provides the best performance. The reason for the reduced improvement in this configuration is explained by the limitation in the number of channels at the output of the array. In both cases, ULA2 and URA4, this number has been set to four, which in the case of the ULA2 allows the use of both channels per antenna, but in the case of the URA4 this limitation forces the receiver to not exploit all the available information. Reducing the number of inputs of the beamforming techniques from eight, which would be the total amount if each antenna exploited both channels, to four, leaves the URA4 configuration with dual-polarization with similar capacities to the dual-polarized ULA2 scheme.

However, as previously stated, the results for the case where polarization diversity is combined with the spatial diversity provided by the array show an improvement of a few dB with respect to the linearly and circularly polarized cases in terms of cancellation capacity, which is also translated in a reduction of the DLL and PLL RMSE. In this case, the DLL error for small delays is not as reduced as in the ULA2 configuration, achieving an improvement of 2-3 meters for very small delays, around $0.2T_c$ and up to 10 meters for delays around $0.5T_c$.
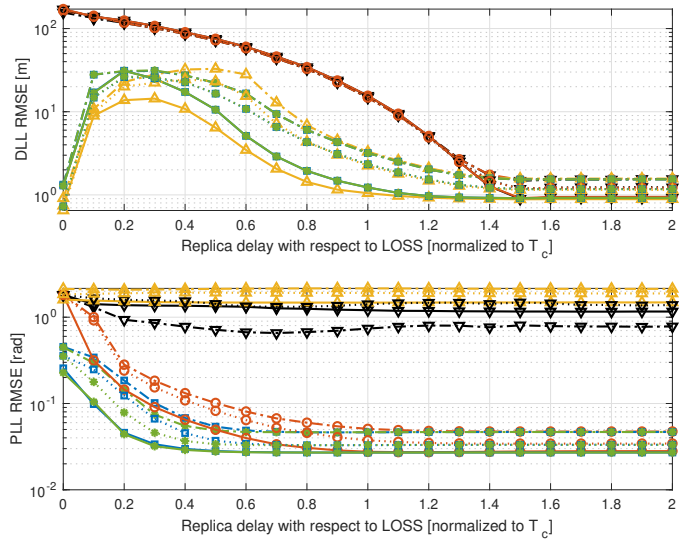
V. CONCLUSION

In this paper, the use of polarization diversity along with spatial diversity has been evaluated for the case of very small antenna arrays, where limitations in both size and complexity prevent the deployment of large antenna arrays. As the mitigation capabilities, and consequently the receiver performance, is contingent on the number of antennas used, the results observed when working with only a few elements are very restricted. In this work, the use of dual-polarized antennas is proposed for small antenna arrays, in order to provide the receiver with an additional domain to exploit from the perspective of multipath mitigation. The results obtained from the simulations performed show that this polarization diversity greatly helps improving the receiver performance, increasing the SMR and reducing the error in the time delay estimation. Particularly, the presented results show that for very limited arrays, as it is the case of the ULA2, introducing dual-polarized antennas considerably enhances the capacity of the receiver to mitigate multipath, providing it with additional robustness even in the case of highly correlated multipath.

REFERENCES

[1] G. A. McGraw and M. S. Braasch, "GNSS multipath mitigation using gated and high resolution correlator concepts," in *Proceedings of the 1999 national technical meeting of the institute of navigation*, 1999, pp. 333–342.

[2] P. D. Groves and Z. Jiang, "Height Aiding, C/N0 Weighting and Consistency Checking for GNSS NLOS and Multipath Mitigation in Urban Areas," *The Journal of Navigation*, vol. 66, no. 5, p. 653–669, 2013.

[3] A. L. Swindlehurst, B. D. Jeffs, G. Seco-Granados, and J. Li, "Applications of Array Signal Processing," in *Academic Press Library in Signal Processing: Volume 3*, ser. Academic Press Library in Signal Processing. Elsevier, 2014, vol. 3, ch. 20, pp. 859–953.

[4] E. G. Larsson, O. Edfors, F. Tufvesson, and T. L. Marzetta, "Massive MIMO for next generation wireless systems," *IEEE Communications Magazine*, vol. 52, no. 2, pp. 186–195, 2014.

[5] F. W. Vook, A. Ghosh, and T. A. Thomas, "MIMO and beamforming solutions for 5G technology," in *2014 IEEE MTT-S International Microwave Symposium (IMS2014)*, 2014, pp. 1–4.

[6] N. O. Parchin, Y. I. A. Al-Yasir, A. H. Ali, I. Elfergani, J. M. Noras, J. Rodriguez, and R. A. Abd-Alhameed, "Eight-Element Dual-Polarized MIMO Slot Antenna System for 5G Smartphone Applications," *IEEE Access*, vol. 7, pp. 15 612–15 622, 2019.

[7] D. Egea-Roca, M. Arizabaleta-Diez, T. Pany, F. Antreich, J. A. López-Salcedo, M. Paonni, and G. Seco-Granados, "GNSS User Technology: State-of-the-Art and Future Trends," *IEEE Access*, vol. 10, pp. 39 939–39 968, 2022.

[8] A. Lehner and A. Steingass, "A novel channel model for land mobile satellite navigation," in *Proceedings of the 18th International Technical Meeting of the Satellite Division of The Institute of Navigation (ION GNSS 2005)*, 2005, pp. 2132–2138.

[9] *Wireless Communications: Principles and Practice*, ser. Prentice Hall communications engineering and emerging technologies series. Dorling Kindersley, 2009. [Online]. Available: https://books.google.es/books?id=11qEWkNFFwQC

[10] R. U. R. Lighari, M. Berg, J. Kallankari, A. Parssinen, and E. T. Salonen, "Analysis of the measured RHCP and LHCP GNSS signals in multipath environment," in *2016 International Conference on Localization and GNSS (ICL-GNSS)*, 2016, pp. 1–6.

[11] M. Berg, R. U. R. Lighari, J. Kallankari, V. Majava, A. Pärssinen, and E. T. Salonen, "Polarization based measurement system for analysis of GNSS multipath signals," in *2016 10th European Conference on Antennas and Propagation (EuCAP)*, 2016, pp. 1–4.

[12] M. Jianguo, C. Kejing, X. Jiangning, and Z. Yinbing, "GPS reflected signal analysis based on software receiver," in *2010 2nd International Conference on Signal Processing Systems*, vol. 2, 2010, pp. V2–176–V2–178.

[13] M. Brenneman, J. Morton, C. Yang, and F. van Graas, "Mitigation of GPS Multipath Using Polarization and Spatial Diversities," in *Proceedings of the 20th International Technical Meeting of the Satellite Division of The Institute of Navigation (ION GNSS 2007)*, 2007, pp. 1221–1229.

[14] F. Fohlmeister, A. Iliopoulos, M. Sgammini, F. Antreich, and J. Nossek, "Dual Polarization Beamforming Algorithm for Multipath Mitigation in GNSS," *Signal Processing*, vol. 138, no. C, p. 86–97, sep 2017. [Online]. Available: https://doi.org/10.1016/j.sigpro.2017.03.012

[15] F. Wendler, F. Antreich, J. A. Nossek, and A. L. Swindlehurst, "Dual-Polarization Time Delay Estimation for Multipath Mitigation," in *WSA 2015; 19th International ITG Workshop on Smart Antennas*, 2015, pp. 1–6.

[16] J. Capon, "High-resolution frequency-wavenumber spectrum analysis," *Proceedings of the IEEE*, vol. 57, no. 8, pp. 1408–1418, 1969.

[17] R. Schmidt, "Multiple emitter location and signal parameter estimation," *IEEE Transactions on Antennas and Propagation*, vol. 34, no. 3, pp. 276–280, 1986.

[18] P. Stoica and K. Sharman, "Maximum likelihood methods for direction-of-arrival estimation," *IEEE Transactions on Acoustics, Speech, and Signal Processing*, vol. 38, no. 7, pp. 1132–1143, 1990.

[19] C. Fernández-Prades, P. Closas, and J. Arribas, "Eigenbeamforming for interference mitigation in GNSS receivers," in *2011 International Conference on Localization and GNSS (ICL-GNSS)*, 2011, pp. 93–97.

[20] A. Konovaltsev, F. Antreich, and A. Hornbostel, "Performance assessment of antenna array algorithms for multipath and interferers mitigation," in *Proc. Workshop on GNSS Signals & Signal Processing (GNSS SIGNALS)*, April 2007.

[21] G. Seco-Granados, J. Fernández-Rubio, and C. Fernández-Prades, "ML estimator and hybrid beamformer for multipath and interference mitigation in GNSS receivers," *IEEE Trans. Signal Process.*, vol. 53, no. 3, pp. 1194–1208, 2005.

[22] M. Mañosas-Caballú, A. L. Swindlehurst, and G. Seco-Granados, "Power-based Capon beamforming: Avoiding the cancellation effects of GNSS multipath," *Signal Process.*, vol. 180, pp. 1–9, 2021.

[23] ETSI, "TS 103 246-3 - Satellite Earth stations and systems (SES); GNSS based location systems; Part 3: Performance requirements," October 2020.